Inorg. Chem. **2006**, *45*, 6308–6316

Crystal Structures and Magnetic and Luminescent Properties of a Series of Homodinuclear Lanthanide Complexes with 4-Cyanobenzoic Ligand

Yan Li,[†,‡] Fa-Kun Zheng,*[,†] Xi Liu,[†,‡] Wen-Qiang Zou,[†,‡] Guo-Cong Guo,*[,†] Can-Zhong Lu,[†] and Jin-Shun Huang[†]

State Key Laboratory of Structural Chemistry, Fujian Institute of Research on the Structure of Matter, Chinese Academy of Sciences, Fuzhou, Fujian 350002, P. R. China, and Graduate School, Chinese Academy of Sciences, Beijing 100039, P. R. China

Received February 15, 2006

A series of homodinuclear lanthanide(III) complexes with the 4-cba ligand, $[La_2(4\text{-cba})_6(phen)_2(H_2O)_6]$ (**1**) and $[Ln_2(4\text{-cba})_6(phen)_2(H_2O)_2]$ (Ln = Pr (**2**), Nd (**3**), Sm (**4**), Eu (**5**), Gd (**6**), and Dy (**7**); 4-Hcba = 4-cyanobenzoic acid; phen = 1,10-phenanthroline), have been synthesized and structurally characterized by single-crystal *X*-ray diffraction. In **1**, two water molecules bridge two nine-coordinated La ions, and six 4-cba ligands coordinate to the two La ions in terminal mode. In the isostructural complexes **2**–**7**, two eight-coordinated Ln ions are connected by four bidentate 4-cba ligands, and another two 4-cba ligands terminate the two Ln ions. The variable-temperature magnetic properties of **2**–**7** have been investigated. Complex **7** shows a significant ferromagnetic interaction between Dy(III), while no magnetic interaction exists between Gd(III) ions in **6**. In **2**–**5**, the value of $\chi_M T$ decreases with decreasing temperature, but the magnetic interactions between the Ln(III) ions cannot definitely be concluded. Notably, the spin–orbit coupling parameters, λ, for Sm(III) (216(2) cm^{-1}) and Eu(III) (404(2) cm^{-1}) have been obtained in **4** and **5**, respectively. The strong fluorescent emissions of **4**, **5**, and **7** demonstrate that ligand-to-Ln(III) energy transfer is efficient and that the coordinated water molecules do not quench their luminescence by the nonradiative dissipation of energy.

Introduction

The chemistry of lanthanide complexes is currently of great interest because of their unique physicochemical properties and various applications as functional materials.[1] Especially, the magnetic[2] and luminescent properties[3] of lanthanide complexes have aroused much attention for decades. In the magnetism area, lanthanide ions with large spin moments should be natural choices for molecular magnetic materials, but in most of these systems the small exchange-coupling constants are problematic:[4] this is the result of the 4f orbitals being very efficiently shielded by the fully occupied 5s and 5p orbitals and thus almost uninvolved in bonds between neighboring lanthanide ions. In addition, the large orbital contributions of most of lanthanide ions and the effects of the crystal field, which make the explanation for the nature

* To whom correspondence should be addressed. E-mail: zfk@fjirsm.ac.cn (F.-K.Z.); gcguo@ms.fjirsmac.cn (G.-C.G.).

† Fujian Institute of Research on the Structure of Matter, Chinese Academy of Sciences.

‡ Graduate School of Chinese Academy of Sciences.

(1) (a) Yan, B.; Zhang, H. J.; Wang, S. B.; Ni, J. Z. *Mater. Res. Bull.* **1998**, *33*, 1517. (b) de Sá, G. F.; Malta, O. L.; de Mello Donegá, C.; Simas, A. M.; Longo, R. L.; Santa-Cruz, P. A.; da Silva, E. F., Jr. *Coord. Chem. Rev.* **2000**, *196*, 165. (c) Vicentini, G.; Zinner, L. B.; Zukerman-Schpector, J.; Zinner, K. *Coord. Chem. Rev.* **2000**, *196*, 353. (d) Kido, J.; Okamoto, Y. *Chem. Rev.* 2002, 102, 2357.

(2) (a) Kido, T.; Ikuta, Y.; Sunatsuki, Y.; Ogawa, Y.; Matsumoto, N. *Inorg. Chem.* **2003**, *42*, 398. (b) Figuerola, A.; Diaz, C.; Ribas, J.; Tangoulis, V.; Granell, J.; Lloret, F.; Mahía, J.; Maestro, M. *Inorg. Chem.* **2003**, *42*, 641. (c) Caneschi, A.; Dei, A.; Gatteschi, D.; Sorace, L.; Vostrikova, K. *Angew. Chem., Int. Ed.* **2000**, *39*, 246. (d) Zhao, H.; Bazile, M. J.; Galán-Mascarós, J. R.; Dunbar, K. R. *Angew. Chem., Int. Ed.* **2003**, *42*, 1015. (e) Hatscher, S. T.; Urland, W. *Angew. Chem., Int. Ed.* **2003**, *42*, 2862. (f) Ishikawa, N.; Otsuka, S.; Kaizu, Y. *Angew. Chem., Int. Ed.* **2005**, *44*, 731.

(3) (a) Yang, C.; Fu, L. M.; Wang, Y.; Zhang, J. P.; Wong, W. T.; Ai, X. C.; Qiao, Y. F.; Zou, B. S.; Gui, L. L. *Angew. Chem., Int. Ed.* **2004**, *43*, 5010. (b) Pope, S. J. A.; Coe, B. J.; Faulkner, S.; Bichenkova, E. V.; Yu, X.; Douglas, K. T. *J. Am. Chem. Soc.* **2004**, *124*, 9490. (c) Liu, W. S.; Jiao, T. Q.; Li, Y. Z.; Liu, Q. Z.; Tan, M. Y.; Wang, H.; Wang, L. F. *J. Am. Chem. Soc.* **2004**, *126*, 2280. (d) Fu, L. M.; Wen, X. F.; Ai, X. C.; Sun, Y.; Wu, Y. S.; Zhang, J. P.; Wang, Y. *Angew. Chem., Int. Ed.* **2005**, *44*, 747.

(4) (a) Costes, J. P.; Nicodème F. *Chem.—Eur. J.* **2002**, *8*, 3442. (b) Ishikawa, N.; Iino, T.; Kaizu, Y. *J. Am. Chem. Soc.* **2002**, *124*, 11440.

10.1021/ic0602603 CCC: $33.50
Published on Web 07/08/2006

and magnitude of f−f interactions very difficult, embarrass the study of lanthanide magnetic property in a way. Recently, Ishikawa and co-workers proposed a new method to determine the crystal-field parameters for a series of dinuclear phthalocyanine lanthanide complexes,[4b,5] bringing some light on this field. However, in contrast with the explanation for the occurrence of ferro- or antiferromagnetic exchange for transition metal ions,[6] the situation for lanthanide ions is less advanced, and the f−f interactions are much less investigated.[4,7] To further explore this field, another good choice is to choose the homodinuclear complexes as good models because they can provide valuable information regarding f−f magnetic exchange.

Aromatic carboxylate coordination complexes, possessing special physical properties and intriguing structural features, have attracted increasing interest.[8] In the reported complexes, it has been proven by the aromatic carboxylate ligands supporting significant magnetic interactions between the lanthanide(III) ions[7e,9] and supporting the strong lanthanide-(III)-centered luminescent emission.[10] In the above context, we select 4-cyanobenzoic acid (4-Hcba) and 3-cyanobenzoic acid (3-Hcba) with two coordination groups and an electron-conjugated system to bind metal atoms to produce new complexes, which may have novel magnetic and optical properties. Compared to other carboxylic acids, the chemistry of Hcba has only been investigated in a limited manner so far.[11] Our previous studies have mainly focused on transition metal complexes with the Hcba ligand.[12] Recently, we employed 4-Hcba and 1,10-phenanthroline, as mixed ligands, and synthesized a series of homodinuclear lanthanide complexes, $[La_2(4\text{-cba})_6(phen)_2(H_2O)_6]$ **1** and $[Ln_2(4\text{-cba})_6(phen)_2(H_2O)_2]$, where Ln = Pr (**2**), Nd (**3**), Sm (**4**), Eu (**5**), Gd (**6**), and Dy (**7**). Here, we report their syntheses, structures, and magnetic and optical properties. It is worth noting that the lanthanide complexes with the 4-cba ligand have not been exploited.

Experimental Section

Materials and Instrumentation. All chemicals except $Ln(NO_3)_3{\cdot}nH_2O$ and Na(4-cba) were obtained from commercial sources and used without further purification. A series of $Ln(NO_3)_3{\cdot}nH_2O$ compounds were prepared by the reaction of Ln_2O_3 and nitric acid in aqueous solution. The sodium salt of 4-Hcba, Na(4-cba), was prepared by the reaction of 4-Hcba and NaOH in an equivalent molar ratio in hot ethanol. Elemental analyses were performed on a Vario EL III elemental analyzer. The FT-IR spectra were obtained on a Perkin-Elmer Spectrum using KBr disks in the range of 4000−400 cm^{-1}. The magnetic susceptibilities of the title complexes were measured with a Quantum Design MPMS-5S superconducting quantum interference device (SQUID) magnetometer in the temperature range of 2−300 K at a field of 1000 Oe, and diamagnetic corrections were made using Pascal's constants. Photoluminescence analyses were performed on an Edinburgh Instrument F920 fluorescence spectrometer. All powder X-ray diffraction data were collected using Rigaku Dmax2500PC powder diffractometer (Cu Kα radiation; $5° \le 2\theta \le 60°$).

Preparation of 1−7. A mixture of $Ln(NO_3)_3{\cdot}nH_2O$ (0.3 mmol), 4-cba (0.6 mmol), and phen (0.5 mmol) in a mixed solution of ethanol (10 mL) and water (5 mL) was sealed into a 25 mL poly(tetrafluoroethylene)-lined stainless steel container under autogenous pressure and then heated at 100 °C for 3 days and cooled to 30 °C at 1 °C h^{-1}. Prismatic single crystals suitable for X-ray analyses were obtained by slow evaporation of the solvent after a few days. Yield: 40% (based on La) for **1**; 45% (based on Pr) for **2**; 70% (based on Nd) for **3**; 65% (based on Sm) for **4**; 50% (based on Eu) for **5**; 75% (based on Gd) for **6**; 55% (based on Dy) for **7**. Anal. Calcd for **1**: C, 53.26; H, 3.23; N, 8.63. Found: C, 53.90; H, 3.01; N, 8.22. Anal. Calcd for **2**: C, 55.59; H, 2.85; N, 9.01. Found: C, 55.23; H, 2.95; N, 9.09. Anal. Calcd for **3**: C, 55.52; H, 2.85; N, 9.00. Found: C, 55.38; H, 2.99; N, 8.86. Anal. Calcd for **4**: C, 54.82; H, 2.81; N, 8.88. Found: C, 54.71; H, 2.95; N, 8.86. Anal. Calcd for **5**: C, 54.75; H, 2.81; N, 8.87. Found: C, 54.35; H, 2.89; N, 8.47. Anal. Calcd for **6**: C, 54.40; H, 2.79; N, 8.82. Found: C, 54.16; H, 2.95; N, 8.79. Anal. Calcd for **7**: C, 53.99; H, 2.77; N, 8.75. Found: C, 54.11; H, 2.81; N, 8.73. IR (KBr, cm^{-1}): for **1** 3441 (br), 2924 (m), 2853 (w), 2234 (s, ν (CN)), 1600 (s, ν_{asym} (CO_2)), 1589 (s, ν_{asym} (CO_2)), 1554 (s), 1520 (w), 1426 (s, ν_{sym} (CO_2)), 1404 (vs, ν_{sym} (CO_2)), 1356 (m), 1290 (w), 1142 (w), 1103 (w), 1020 (w), 874 (w), 848 (w), 788 (m), 729 (m), 697 (w), 667 (w), 569 (m), 546 (w); for **2** 3437 (br), 2922 (w), 2852 (w), 2228 (s, ν (CN)), 1623 (s, ν_{asym} (CO_2)), 1590 (s, ν_{asym} (CO_2)), 1549 (s), 1516 (m), 1426 (s, ν_{sym} (CO_2)), 1406 (vs, ν_{sym} (CO_2)), 1346 (m), 1293 (m), 1142 (w), 1102 (w), 1018 (w), 864 (m), 844 (m), 780 (s), 728 (m), 693 (m), 637 (w), 566 (m), 545 (m); for **3** 3436 (br),

(5) (a) Ishikawa, N.; Iino, T.; Kaizu, Y. *J. Phys. Chem. A* **2002**, *106*, 9543. (b) Ishikawa, N.; Iino, T.; Kaizu, Y. *J. Phys. Chem. A* **2003**, *107*, 7879. (c) Ishikawa, N.; Sugita, M.; Okubo, T.; Tanaka, N.; Iino, T.; Kaizu, Y. *Inorg. Chem.* **2003**, *42*, 2440.

(6) Kahn, O. *Molecular Magnetism*; VCH: New York, 1993.

(7) (a) Liu, S.; Celmini, L.; Rettig, S. J.; Thompson, R. C.; Orvig, C. *J. Am. Chem. Soc.* **1992**, *114*, 6081. (b) Panagiotopoulos, A.; Zafiropoulos, T. F.; Perlepes. S. P.; Bakalbassis, E.; Masson-Ramade, I.; Kahn, O.; Terzis, A.; Raptopoulou, C. P. *Inorg. Chem.* **1995**, *34*, 4, 4918. (c) Ma, B. Q.; Zhang, O. S.; Gao, S.; Jin, T. Z.; Yan, C. H.; Xu, G. X. *Angew. Chem., Int. Ed.* **2000**, *39*, 3644. (d) Costes, J. P.; Dahan, F.; Nicodème, F. *Inorg. Chem.* **2001**, *40*, 5285. (e) Costes, J. P.; Clemente-Juan, J. M.; Dahan, F.; Nicodème, F.; Verelst, M. *Angew. Chem., Int. Ed.* **2002**, *41*, 323. (f) Wan, Y. L.; Zhang, L. P.; Jin, L. P.; Gao, S.; Lu, S. Z. *Inorg. Chem.* **2003**, *42*, 4985. (g) Gheorghe, R.; Kravtsov, V.; Simonov, Y. A.; Costes, J. P.; Journaux, Y.; Andruh, M. *Inorg. Chim. Acta* **2004**, *357*, 1613. (h) Zheng, X. J.; Wang, Z. M.; Gao, S.; Liao, F. H.; Yan, C. H.; Jin, L. P. *Eur. J. Inorg. Chem.* **2004**, 2968. (i) Zhang, H. T.; Song, Y.; Li, Y. X.; Zuo, J. L.; Gao, S.; You, X. Z. *Eur. J. Inorg. Chem.* **2005**, 766.

(8) (a) Eddaudi, M.; Kim, J.; Wachter, J. B.; Chae, H. K.; O'Keeffe, M.; Yaghi, O. M. *J. Am. Chem. Soc.* **2001**, *123*, 4368. (b) Eddaoudi, M.; Kim, J.; Rosi, N.; Vodak, D.; Wachter, J.; O'Keeffe, M.; Yaghi, O. M. *Science* **2002**, *295*, 469. (c) Pan, L.; Sander, M. B.; Huang, X.; Li, J.; Smith, M.; Bittner, E.; Bockrath, B.; Johnson, J. K. *J. Am. Chem. Soc.* **2004**, *126*, 1308.

(9) Costes, J. P.; Clemente Juan, J. M.; Dahan, F.; Nicodème, F. *J. Chem. Soc., Dalton Trans.* **2003**, 1272.

(10) (a) Reineke, T. M.; Eddaoudi, M.; Fehr, M.; Yaghi, O. M. *J. Am. Chem. Soc.* **1999**, *121*, 1, 1651. (b) Dias, A. B.; Viswanathan, S. *Chem. Commun.* **2004**, 1024.

(11) (a) Schiavo, S. L.; NicolÒ, F.; Tresoldi, G.; Piraino, P. *Inorg. Chim. Acta* **2003**, *343*, 351. (b) Yuan, R. X.; Xiong, R. G.; Chen, Z. F.; You, X. Z.; Peng, S. M.; Lee, G. H. *Inorg. Chem. Commun.* **2001**, *4*, 430. (c) Keys, A.; Bott, S. G.; Barron, A. R. *Polyhedron* **1998**, *17*, 3121. (d) Ma, B. Q.; Gao, S.; Wang, Z. M.; Yi, T.; Yan, C. H.; Xu, G. H. *Acta Crystallogr.* **1998**, *C55*, 1420. (e) Cueto, S.; Rys, P.; Straumann, H. P. *Acta Crystallogr.* **1992**, *C48*, 2122.

(12) (a) Zheng, F. K.; Wu, A. Q.; Li, Y.; Guo, G. C.; Wang, M. S.; Li, Q.; Huang, J. S. *J. Mol. Struct.* **2005**, *740*, 147. (b) Li, Y.; Wu, A. Q.; Zheng, F. K.; Fu, M. L.; Guo, G. C.; Huang, J. S. *Inorg. Chem. Commun.* **2005**, *8*, 708. (c) Wang, M. S.; Cai, L. Z.; Zhou, G. W.; Guo, G. C.; Huang, J. S. *Inorg. Chem. Commun.* **2003**, *6*, 855. (d) Li, Y.; Wu, A. Q.; Zheng, F. K.; Guo, G. C.; Lu, C. Z.; Huang, J. S. *Chinese J. Struct. Chem.* **2005**, *24*, 1281. (e) Zheng, F. K.; Zhang X.; Guo, G. C.; Huang, J. S. *Chinese J. Struct. Chem.* **2001**, *20*, 391.

2924 (w), 2853 (w), 2228 (s, ν (CN)), 1624 (s, ν_{asym} (CO_2)), 1590 (s, ν_{asym} (CO_2)), 1549 (s), 1516 (m), 1426 (s, ν_{sym} (CO_2)), 1408 (vs, ν_{sym} (CO_2)), 1346 (w), 1293 (m), 1143 (w), 1102 (w), 1018 (w), 856 (m), 844 (m), 781 (s), 728 (m), 693 (m), 637 (w), 567 (m), 545 (m); for **4** 3441 (br), 2924 (w), 2854 (w), 2228 (s, ν (CN)), 1627 (s, ν_{asym} (CO_2)), 1590 (s, ν_{asym} (CO_2)), 1550 (s), 1517 (m), 1426 (s, ν_{sym} (CO_2)), 1407 (vs, ν_{sym} (CO_2)), 1346 (m), 1293 (m), 1143 (w), 1103 (w), 1018 (w), 865 (m), 843 (m), 780 (s), 728 (m), 693 (m), 638 (w), 567 (m), 545 (m); for **5** 3452 (br), 3079 (w), 2927 (w), 2229 (s, ν (CN)), 1633 (s, ν_{asym} (CO_2)), 1591 (s, ν_{asym} (CO_2)), 1550 (s), 1518 (m), 1426 (s, ν_{sym} (CO_2)), 1409 (vs, ν_{sym} (CO_2)), 1346 (m), 1293 (m), 1143 (w), 1103 (w), 1018 (w), 865 (m), 844 (m), 781 (s), 728 (m), 693 (m), 638 (w), 567 (m), 546 (w); for **6** 3443 (br), 3078 (w), 2920 (w), 2228 (s, ν (CN)), 1631 (s, ν_{asym} (CO_2)), 1590 (s, ν_{asym} (CO_2)), 1550 (s), 1517 (m), 1425 (vs, ν_{sym} (CO_2)), 1410 (vs, ν_{sym} (CO_2)), 1346 (m), 1293 (m), 1143 (w), 1103 (w), 1018 (w), 865 (m), 843 (m), 780 (s), 728 (m), 693 (m), 638 (w), 568 (m), 545 (w); for **7** 3451 (br), 2924 (w), 2852 (w), 2229 (s, ν (CN)), 1635 (s, ν_{asym} (CO_2)), 1591 (s, ν_{asym} (CO_2)), 1551 (s), 1517 (m), 1426 (vs, ν_{sym} (CO_2)), 1410 (vs, ν_{sym} (CO_2)), 1346 (m), 1293 (m), 1143 (w), 1102 (m), 1018 (w), 866 (m), 843 (m), 780 (s), 728 (m), 693 (m), 638 (w), 568 (m), 545 (w). The most characteristic peaks of IR (KBr) for Na(4-cba): 2232 (s, ν (CN)), 1591 (s, ν_{asym} (CO_2)), 1548 (s, ν_{asym} (CO_2)), 1415 (sh, ν_{sym} (CO_2)), 1403 (vs, ν_{sym} (CO_2)) cm^{-1}.

Single-Crystal Structure Determination. The crystal structures of the complexes were studied by single-crystal X-ray diffraction analyses on a Rigaku Mercury CCD diffractometer equipped with graphite-monochromated Mo Kα radiation ($\lambda = 0.71073$ Å) at 293(2) K. The intensity data sets were collected with the ω scan technique and reduced by CrystalClear software.[13] The structures were solved by the direct methods and refined by full-matrix least-squares techniques. Non-hydrogen atoms were located by difference Fourier maps and subjected to anisotropic refinement. The hydrogen atoms of the water molecule were located in difference Fourier syntheses and refined with O−H distances restrained to a target value of 0.96 Å and $U_{iso}(H) = 1.2U_{eq}(O)$, and the remaining hydrogen atoms were calculated in idealized positions and allowed to ride on their parent atom. All of the calculations were performed by the Siemens SHELXTL, version 5, package of crystallographic software.[14] Pertinent crystal data and structure refinement results for the complexes are listed in Table 1.

Results and Discussions

Description of the Structures. The X-ray crystallography analyses revealed that **2**−**7** are isomorphous, so we will choose **1** and **2** for detailed structural discussions.

$[La_2(4\text{-cba})_6(phen)_2(H_2O)_6]$ (1). As shown in Figure 1, the molecule of **1** consists of a centrosymmetric dimeric $[La_2O_2]$ unit. The two La(III) atoms are bridged by two water molecules to generate an ideal parallelogram with a La(III)···La(III) distance of 4.5826(6) Å. The La(III) atom is nine-coordinate, with three O atoms from three 4-cba, two N atoms from one chelating phen molecule, and four coordinated water molecules, to form a distorted monocapped square antiprismatic coordination geometry (Figure S1). One of the quadrangular faces is defined by one carboxylate oxygen atom and three water oxygen atoms (O1W, O3WA, O11, and O3W; symmetry code A $-x, -y, -z$) with a mean deviation of 0.197 Å from the least-squares plane; the other one, which is capped by one nitrogen atom (N2) from one phen molecule, is defined by two oxygen atoms from two crystallographically unique 4-cba ligands, one nitrogen atom from the phen molecule and one coordinated water oxygen atom (O2W, N1, O31, and O21) with a mean deviation of 0.0319 Å from the least-squares plane. The dihedral angle between the two square faces is ca. 1.89(4)°. The La−N distances are in the range of 2.723(2)−2.743(2) Å, in agreement with those of the La(III) analogue with the phen ligands,[15] while the La−O distances are in the range of 2.458(2) and 2.743(2) Å; the longest La−O bonds involve the bridging water oxygen atoms (La1−O3W = 2.743(2) Å, La−O3WA = 2.632(2) Å; symmetry code A $-x, -y, -z$), which are comparable to those found in the $La_2(C_5H_4NCO_2)_6 \cdot (H_2O)_4$ complexes.[16]

Carboxylate groups exhibit only one coordination mode: a terminal monodentate ligand. There are intramolecular hydrogen bonds (O1W···O32A = 2.799(3) Å, O1W−H1WA···O32A = 137(3)°; symmetry code A $-x, -y, -z$), and the dimeric molecules are also connected by intermolecular hydrogen bonds to give a one-dimensional (1D) chain network along the *a* direction with distances of O1W···O21B = 2.940(3) Å, O2W···O22B = 2.746(3) Å, and O2W···O32B = 2.750(3) Å and angles of O1W−H1WB···O21B = 163(3)°, O2W−H2WA···O22B = 173(3)°, and O2W−H2WB···O32B = 162(3)° (symmetry code B $1 + x, y, z$), as depicted in Figure S2. Despite the existence of the terminal monodentate 4-cba ligand, all four C−O distances of two crystallographically independent carboxylate groups involved with hydrogen bonds are almost equal (1.254(3)−1.265(3) Å). Another carboxylate group is not concerned with hydrogen bonds, and its $C-O_{(coordinated)}$ distance (1.282(3) Å) is certainly slightly longer than the $C-O_{(uncoordinated)}$ distances (1.233(3) Å). The nearest separation of La(III)···La(III) through hydrogen bonds is 6.9971(1) Å, which is obviously longer than that through the bridging water oxygen atoms.

$[Ln_2(4\text{-cba})_6(phen)_2(H_2O)_2]$ (2−7). Figure 2 shows the molecular structure of **2**. The molecular entity comprises a center-related dinuclear $[Pr_2(CO_2)_4]$ unit. Four carboxylate groups link a pair of Pr(III) atoms in the O,O′-bridging mode to generate a paddle-wheel-like centrosymmetric dimer [Pr_2(carboxylate-O,O′)$_4$] with Pr(III)···Pr(III) distances of 4.4018(9) Å. The Pr(III) atom is coordinated by four O atoms from four bridging 4-cba ligands, one O atom from a monodentate 4-cba, two N atoms from one chelating phen molecule, and one coordinated water molecule. These eight coordination atoms form a distorted square antiprism (Figure S3). One of the quadrangular faces is defined by two nitrogen atoms from one phen molecule, one terminal carboxylate oxygen atom, and one water oxygen atom (N1, N2, O1W, and O31) with the mean deviation of 0.168 Å from the least-squares plane;

(13) *CrystalClear*, version 1.35; Software User's Guide for the Rigaku R-Axis and Mercury and Jupiter CCD Automated X-ray Imaging System; Rigaku Molecular Structure Corporation: The Woodlands, TX, 2002.
(14) *SHELXTL Reference Manual*, version 5; Siemens Energy & Automation Inc.: Madison, WI, 1994.
(15) Zheng, X. J.; Jin, L. P. *J. Mol. Struct.* **2003**, *655*, 7.
(16) Moore, J. W.; Glick, M. D.; Baker, W. A., Jr. *J. Am. Chem. Soc.* **1972**, *94*, 1858.

Table 1. Crystal Data and Structure Refinement for Complexes **1**−**7**

	1	**2**	**3**	**4**
formula	$C_{72}H_{52}La_2N_{10}O_{18}$	$C_{72}H_{44}Pr_2N_{10}O_{14}$	$C_{72}H_{44}Nd_2N_{10}O_{14}$	$C_{72}H_{44}Sm_2N_{10}O_{14}$
fw	1623.06	1554.99	1561.65	1573.87
cryst dimensions (mm)	0.18, 0.16, 0.10	0.32, 0.20, 0.10	0.25, 0.15, 0.10	0.20, 0.18, 0.08
shape	prism	prism	prism	prism
color	colorless	pale green	pale purple	pale yellow
space group	$P\bar{1}$	$P\bar{1}$	$P\bar{1}$	$P\bar{1}$
a (Å)	6.99710(10)	8.308(2)	8.297(5)	8.2827(8)
b (Å)	14.33860(10)	12.852(4)	12.813(7)	12.8027(11)
c (Å)	18.9494(2)	16.419(5)	16.426(9)	16.4241(15)
α (deg)	108.363(8)	97.443(4)	97.527(4)	97.762(2)
β (deg)	97.397(7)	101.952(4)	102.014(7)	102.084(4)
γ (deg)	103.890(7)	99.497(2)	99.572(6)	99.682(4)
V (Å^3)	1707.96(3)	1667.2(8)	1659.1(16)	1652.4(3)
Z	1	1	1	1
ρ (g/cm^3)	1.578	1.549	1.563	1.582
μ (mm^{-1})	1.314	1.518	1.622	1.834
F(000)	812	776	778	782
θ range (deg)	3.01−25.02	3.17−25.03	3.17−25.03	3.14−25.03
reflns (measured)	10854	10571	10594	10601
R_{int}	0.0190	0.0180	0.0312	0.0281
data (obsd)/restraints/params	5639/6/473	5532/14/448	5305/2/450	5305/2/448
R_1, R_2 (obsd)	0.0285, 0.0617	0.0273, 0.0676	0.0390, 0.0907	0.0371, 0.0866
GOF on F^2	1.004	1.004	1.003	1.002
largest and mean δ/σ	0.000, 0.000	0.003, 0.000	0.015, 0.000	0.000, 0.000
largest difference peak (e Å^3)	1.051, −0.394	0.539, −0.500	0.327, −0.248	0.484, −0.485

	5	**6**	**7**
formula	$C_{72}H_{44}Eu_2N_{10}O_{14}$	$C_{72}H_{44}Gd_2N_{10}O_{14}$	$C_{72}H_{44}Dy_2N_{10}O_{14}$
fw	1577.09	1587.67	1598.17
cryst dimensions (mm)	0.38, 0.30, 0.10	0.40, 0.23, 0.10	0.38, 0.25, 0.10
shape	prism	prism	prism
color	colorless	colorless	colorless
space group	$P\bar{1}$	$P\bar{1}$	$P\bar{1}$
a (Å)	8.2745(6)	8.273(2)	8.2525(7)
b (Å)	12.8076(9)	12.796(4)	12.7935(12)
c (Å)	16.4256(13)	16.424(5)	16.4146(12)
α (deg)	97.838(2)	97.903(2)	97.941(3)
β (deg)	102.116(3)	102.136(3)	102.068(2)
γ (deg)	99.720(3)	99.775(3)	99.918(4)
V (Å^3)	1650.6(2)	1647.9(8)	1641.9(2)
Z	1	1	1
ρ (g/cm^3)	1.587	1.600	1.616
μ (mm^{-1})	1.957	2.070	2.333
F(000)	784	786	790
θ range (deg)	3.14−25.03	3.14−25.03	3.18−25.03
reflns (measured)	10510	10447	10387
R_{int}	0.0203	0.0168	0.0168
data (obsd)/constraints/params	5399/2/448	5446/2/448	5432/2/448
R_1, R_2 (obsd)	0.0269, 0.0644	0.0234, 0.0589	0.0232, 0.0583
GOF on F^2	1.007	1.002	1.006
largest and mean δ/σ	0.000, 0.000	0.001, 0.000	0.000, 0.000
largest difference peak (e Å^3)	0.441, −0.493	0.407, −0.641	0.408, −0.972

the other one is defined by four oxygen atoms from two crystallographically unique 4-cba ligand (O11, O12A, O21, and O22A; symmetry code A $1 - x, -y, 1 - z$) with a negligible mean deviation of 0.0005 Å from the least-squares plane. The dihedral angle between the square faces is ca. 21.27(9)°, reflecting the distorted square antiprism. The bond distances of Pr−N (Pr1−N1 = 2.661(3) Å, Pr1−N2 = 2.675(3) Å are comparable to those of the previously reported phen-containing Pr(III) complex.[17] The Pr−O bond distances fall in range of 2.405(2)−2.481(2) Å, which are similar to those of the Pr(III) analogue.[18,19]

The carboxylate groups are bound to the Pr(III) ions in three different coordination fashions: a common monodentate mode, a bidentate bridging mode in the syn−syn configuration, as well as an unusual bidentate bridging coordination mode in the syn−anti configuration, which, to the best our knowledge, has not been encountered in 4-cba complexes.

Likewise, supramolecular interactions also play an important role in the crystal packing and stabilization of **2**. There is a concurrence of hydrogen bonds and $\pi-\pi$ stacking interactions. First, there are strong intramolecular hydrogen bonds resulting from the coordinated water molecule and uncoordinated carboxylate O atom (O1W···O32 = 2.618(3) Å and O1W−H1WB···O32 = 162(3)°). Second, as shown in Figure S4, face-to-face $\pi-\pi$ stacking interactions between rings R1 (atoms C1, C2, C3 C4, C12, and N1) and

(17) Dong, N.; Zhu, L. G.; Xu, C. *Chinese J. Struct. Chem.* **1993**, *12*, 133.
(18) Xu, H. T.; Zheng, N. W.; Jin, X. L.; Yang, R. Y.; Wu, Y. G.; Ye, E. Y.; Li, Z. Q. *J. Mol. Struct.* **2003**, *655*, 339.
(19) Junk, P. C.; Kepert, C. J.; Lu, W. M.; Skelton, B. W.; White, A. H. *J. Aust. J. Chem.* **1999**, *52*, 459.

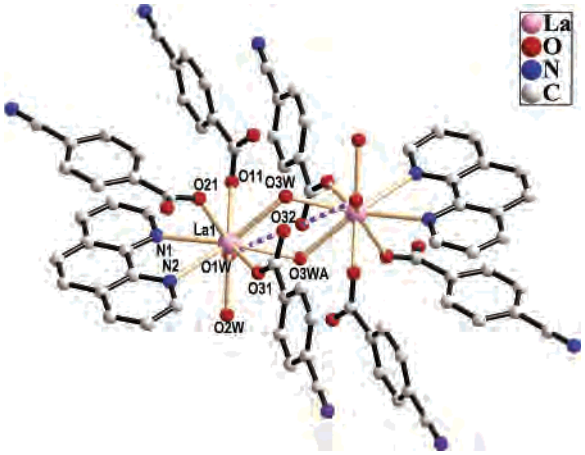

Figure 1. Molecular structure of **1**. All hydrogen atoms are omitted for clarity, and the dashed line represents the intramolecular hydrogen bonds.

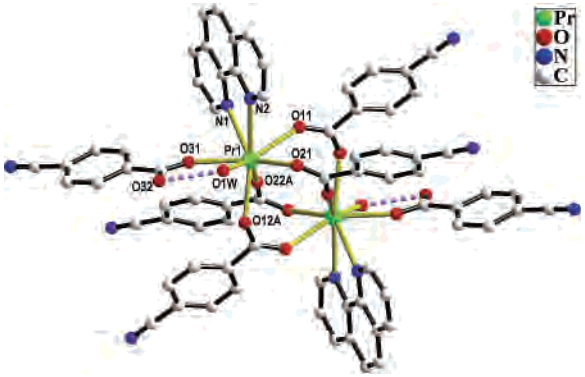

Figure 2. Molecular structure of **2**. All hydrogen atoms are omitted for clarity, and the dashed line represents the intramolecular hydrogen bonds.

R2 (atoms C4, C5, C6, C7, C11, and C12) from neighboring phen molecules, with a dihedral angle of 2.3(2)° and a centroid-to-centroid distance of 3.755 Å, generate a 1D chained network along the *b* direction. The adjacent chains are further connected to form a two-dimensional (2D) network parallel to the *ab* plane through $\pi-\pi$ stacking between rings R2 and R3 (atoms C7, C8, C9, C10, N2, and C11) from the adjacent-chain phen molecules, with a dihedral angle of 2.5(2)° and a centroid-to-centroid distance of 3.646 Å. The nearest separation (6.3532(13) Å) of Pr(III)···Pr(III) via $\pi-\pi$ stacking is longer than that via the bridging carboxylate groups.

The range of Ln−$O_{(terminal\ 4-cba)}$, Ln−$O_{(bridging\ 4-cba)}$, Ln−$O_{(water)}$, Ln−N, and Ln···Ln distances are given in Table 2. The dinuclear structures of **2**−**7**, bridged by carboxylate groups, are different from that of **1**, bridged by water oxygen atoms. The Ln(III) atom is eight-coordinate in **2**−**7**, while in **1** the La(III) atom is nine-coordinate. The Ln(III)···Ln-(III) distances of **2**−**7** fall in the range of 4.401(2)−4.4252-(9) Å, which are visibly shorter than that of **1** (4.5826(6) Å). This is because the radius of the La(III) ion is larger than those of other lanthanide(III) ions (namely, lanthanide contraction). Another important reason is the anionic 4-cba ligand has a higher affinity of bonding to the cationic lanthanide ions than the neutral water molecule. As expected, in all complexes, the Ln−O (terminal), Ln−O (bridging), Ln−O (water), and Ln−N distances show a slight and continuous decrease upon going from the larger La(III) to the smaller Dy(III) cation, whereas the change of Ln(III)···Ln(III) distances is not obvious from **2** to **7**.

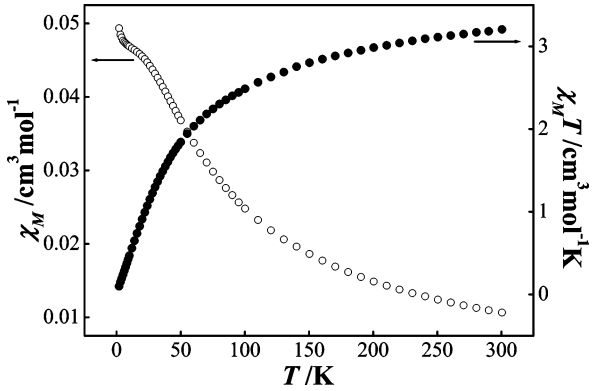

Figure 3. Plots of χ_M and $\chi_M T$ vs T for **2**.

Magnetic Properties. In contrast with the effects of the crystal field, the spin−orbital coupling in general plays a more important role in the magnetism of lanthanide complexes. This large spin−orbit coupling partly removes the degeneracy of the $^{2S+1}$L group term of lanthanide ions, giving $^{2S+1}L_J$ states, which further split into Stark levels by crystal field perturbation. For most of free lanthanide ions, the energy separation between the $^{2S+1}L_J$ ground state and the first excited state is so large that only the ground state is thermally populated at room and low temperature, but this situation is possibly exceptional for the Sm(III) and Eu(III) ions in which the first excited state may be thermally populated because of the weak energy separation. Thus, in the series of dinuclear lanthanide complexes reported here, the crystal field effect must be taken into account and the possible thermal population of the higher states should also be taken into consideration for Sm(III) and Eu(III) complexes.

$[Pr_2(4\text{-cba})_6(phen)_2(H_2O)_2]$ (2). The variable-temperature magnetic susceptibility, χ_M, and $\chi_M T$ are shown in Figure 3. At 300 K, $\chi_M T$ is equal to 3.205 cm^3 K mol^{-1}, as expected for two isolated Pr(III) ions (3.20 cm^3 K mol^{-1}). As the temperature is lowered, the $\chi_M T$ value decreases more and

Table 2. Selected Bond Distances (Å)

	Ln−$O_{(terminal\ 4-cba)}$	Ln−$O_{(bridging\ 4-cba)}$	Ln−$O_{(water)}$	Ln−N	Ln···Ln
1	2.458(2)−2.484(2)		2.577(2)−2.743(2)	2.723(2), 2.743(2)	4.5826(6)
2	2.427(2)	2.405(2)−2.481(2)	2.468(2)	2.661(3), 2.675(3)	4.4018(9)
3	2.415(3)	2.387(3)−2.461(3)	2.454(3)	2.636(4), 2.649(4)	4.401(2)
4	2.387(3)	2.349(3)−2.429(3)	2.432(3)	2.616(4), 2.624(4)	4.4156(6)
5	2.371(2)	2.335(2)−2.417(2)	2.417(2)	2.604(3), 2.612(3)	4.4214(4)
6	2.364(2)	2.325(2)−2.408(2)	2.410(2)	2.590(2), 2.596(3)	4.4252(9)
7	2.342(2)	2.298(2)−2.382(2)	2.387(2)	2.563(2), 2.577(2)	4.4145(4)

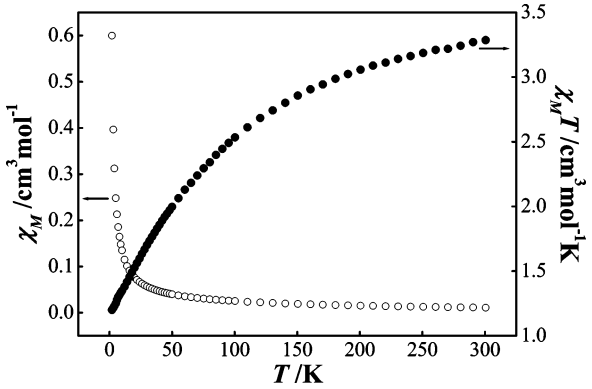

Figure 4. Plots of χ_M and $\chi_M T$ vs T for **3**.

more rapidly and reaches 0.099 cm^3 K mol^{-1} at 2.0 K. However, the whole profile of the $\chi_M T$ versus T curve is not indicative of the nature of the interactions between the two Pr(III) ions because of the crystal-field effect, which splits the 9-fold degenerate $^3H_4$ ground state into Stark levels, and the values of $\chi_M T$ mainly depend on the populations of those Stark levels. At room temperature, all the Stark levels from the 9-fold degenerate $^3H_4$ ground states are populated, such that $\chi_M T$ is equal to the value expected for two free ions, but as the temperature decreases, a progressive depopulation of higher Stark levels occurs, so the value of $\chi_M T$ begins to decrease.

[Nd$_2$(4-cba)$_6$(phen)$_2$(H$_2$O)$_2$] (3). A similar evolution is observed in the case of **3**. As illustrated in Figure 4, $\chi_M T$ is equal to 3.286 cm^3 K mol^{-1} at 300 K, which is consistent with the value expected for two isolated Nd(III) ions (3.28 cm^3 K mol^{-1}), and decreases continuously to a value of 1.200 cm^3 K mol^{-1} at 2 K. This is mainly because of the splitting of the 10-fold degenerate $^4I_{9/2}$ ground state by the crystal field and the progressive depopulation of the higher energy, as the temperature is lowered. Notably, the whole profile of the $\chi_M T$ versus T curve is similar to that reported for mononuclear and homodinuclear complexes.[20] Therefore, even if the magnetic interaction is present, it should be very weak.

[Sm$_2$(4-cba)$_6$(phen)$_2$(H$_2$O)$_2$] (4). The magnetic characteristic of the Sm(III) complex is different from those of the Pr(III) and Nd(III) complexes. The ^6H ground term for the free Sm(III) ions is split into six states by spin−orbit coupling, and the spin−orbit coupling parameter is on the order of 200 cm^{-1}, so both the crystal-field effect and the possible thermal population of the higher states should be evaluated for the Sm(III) complex.

As can be seen from Figure 5, $\chi_M T$ is equal to 0.798 cm^3 K mol^{-1} at 300 K, and decreases rapidly to a value of 0.086 cm^3 K mol^{-1} at 2 K. The thermal variation of $\chi_M T$ is nearly linear over the whole temperature range, which is similar to that for the reported mononuclear complex. But, interestingly, the value of 0.086 cm^3 K mol^{-1} for $\chi_M T$ at 2 K is consistent with the value of 0.089 cm^3 K mol^{-1} predicted by theory for one Sm(III) ion and obviously smaller than that for two

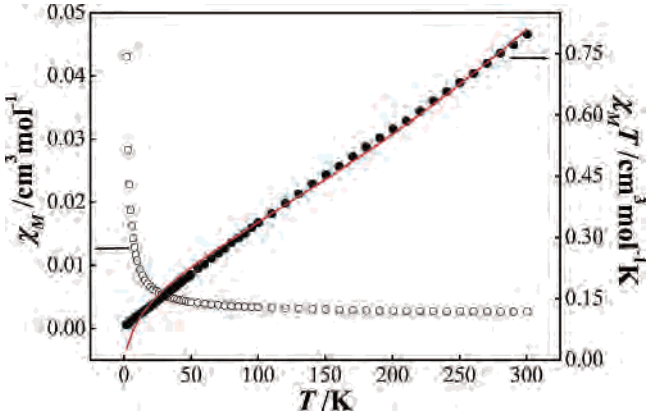

Figure 5. Plots of χ_M and $\chi_M T$ vs T for **4**. The solid line is the calculated curve over the whole temperature range.

Sm(III) ions. This behavior indicates that an antiferromagnetic interaction possibly exists between Sm(III) pairs at low temperature, although it is very weak. The $\chi_M T$ versus T data have been analyzed on the basis of the equations deduced from the Sm(III) ion in a monomeric system with free-ion approximation,[20a] over the whole temperature range. The best agreement between the experimental and calculated data corresponds to the spin−orbit coupling parameter, $\lambda = 216(2)$ cm^{-1}, and the Weiss-like constant, $\theta = -11.32(78)$ K, with an agreement factor R ($R = \sum[(\chi_M T)_{obsd} - (\chi_M T)_{calcd}]^2/\sum(\chi_M T)_{obsd}^2$) of 3.1×10^{-4}. The spin−orbit coupling parameter λ is close to that of the Sm(III) mononuclear complex (193 cm^{-1}), but lower than the value deduced from the spectroscopic data ($\lambda = 281$ cm^{-1} with $J = 7/2$).The deviation of $\chi_M T$ with respect to the equation for the Sm(III) ion with free-ion approximation ($\theta = -11.32(78)$ K) is caused by the crystal field effect, as well as the possible antiferromagnetic interactions between the two Sm(III) ions.

[Eu$_2$(4-cba)$_6$(phen)$_2$(H$_2$O)$_2$] (5). Similar to **4**, the ^7F ground term is split into seven states by spin−orbit coupling, and the energy separation of this states are weak enough that the excited states may be thermally populated at room temperature and above. The $\chi_M T$ versus T data have also been analyzed on the basis of the equations deduced from the Eu(III) ion in the monomeric system with the free-ion approximation,[20a] over the whole temperature range.

The least-squares fitting of the $\chi_M T$ versus T curve leads to $\lambda = 404(2)$ cm^{-1} and $\theta = 1.21(27)$ K with an agreement factor R ($R = \sum[(\chi_M T)_{obsd} - (\chi_M T)_{calcd}]^2/\sum(\chi_M T)_{obsd}^2$) of 3.1×10^{-4}. The spin−orbit coupling parameter λ is slightly larger than that of Eu(III) mononuclear complex (362 cm^{-1}), and comparable to the value (379 cm^{-1}) deduced from the energy difference between the states $^7F_1$ and $^7F_0$, based on the emission spectra (see below discussions on optical spectroscopy).

By comparing the curves of χ_M and $\chi_M T$ versus T of **5** to those of the mononuclear Eu(III) complex, it is interesting to find that they are very similar. As shown in Figure 6, χ_M smoothly increases over the 300−80 K temperature range and then tends to a plateau. Below 25 K, χ_M starts to increases again and more and more rapidly at low temperature, reaching a value of 0.01218 cm^3 mol^{-1}. At 300 K,

(20) (a) Andruh, M.; Bakalbassis, E.; Kahn, O.; Trombe, J. C.; Porcher, P. *Inorg. Chem.* **1993**, *32*, 2, 1616. (b) Hou, H. W.; Li, G.; Li, L. K.; Zhu, Y.; Meng, X. R.; Fan, Y. T. *Inorg. Chem.* **2003**, *42*, 428.

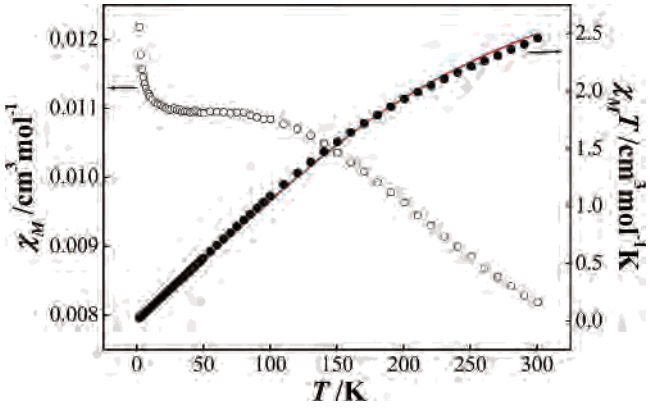

Figure 6. Plots of χ_M and $\chi_M T$ vs T for **5**. The solid line is the calculated curve over the whole temperature range.

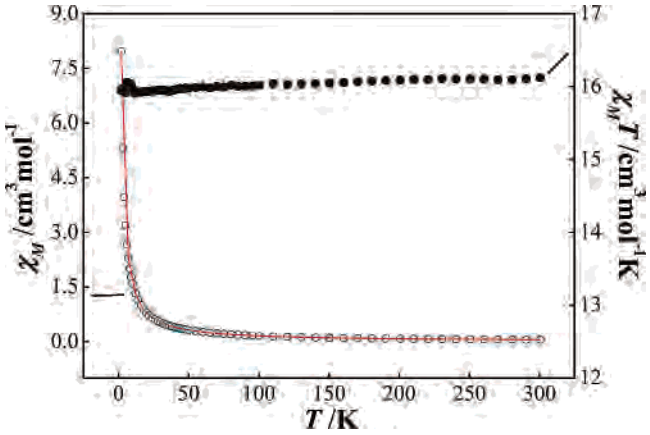

Figure 7. Plots of χ_M and $\chi_M T$ vs T for **6**. The solid line is the calculated curve over the whole temperature range.

$\chi_M T$ is equal to 2.461 cm^3 K mol^{-1}, obviously smaller than the theoretical high-temperature limit $(\chi_M T)_{HT} = 4.50$ cm^3 K mol^{-1}), and it decreased continuously to the value close to zero (0.0244 cm^3 K mol^{-1}) at 2 K. Below 50 K, the thermal variation of $\chi_M T$ is rigorously linear, with the slope $(\chi_M)_{LT} = 0.0109$ cm^{3}mol^{-1}, comparable to the two times that for the mononuclear complex ($(\chi_M)_{LT} = 5.99 \times 10^{-3}$ cm^{3}mol^{-1}). So the magnetic behavior of **5** is mainly caused by single-ion properties, which is also reflected in the small value of the Weiss-like constant θ ($\theta = 1.21(27)$ K).

[Gd$_2$(4-cba)$_6$(phen)$_2$(H$_2$O)$_2$] (6). The situation is simple for **6**. Since Gd(III) has an $^8S_{7/2}$ ground state, which is almost unsplit (0.1 cm^{-1}) and also well separated from the first excited state (about 32 000 cm^{-1}), Gd(III) has a simple spin system as the influence of the crystal field can be neglected.

The thermal variation of the magnetic susceptibility, χ_M, and $\chi_M T$ are shown in Figure 7. $\chi_M T$ is almost constant with small-scale range from 16.12 to 15.94 cm^3 K mol^{-1} over the whole temperature range, which is close to the theoretical value for two isolated Gd(III) (15.86 cm^3 K mol^{-1}).

The almost unchanged value of $\chi_M T$ indicates that there is no interaction between the two Gd(III) ions, which is also reflected in the value of the Weiss constant θ. A nonlinear fit via $\chi_M = C/(T - \theta) + \chi_0$ over the whole temperature range reveals a Curie−Weiss law behavior with a Curie constant, C, of 15.99(1) cm^3 K mol^{-1} and a Weiss constant, θ, of −0.0063(22) K, and the background susceptibility χ_0 $= -2(6) \times 10^{-4}$ cm^3 mol^{-1}. So **6** is paramagnetic, and there is no interaction between Gd(III) ions.

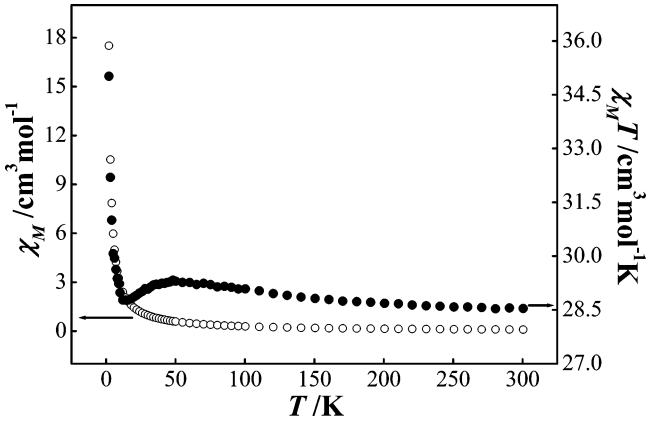

Figure 8. Plots of χ_M and $\chi_M T$ vs T for **7**.

[Dy$_2$(4-cba)$_6$(phen)$_2$(H$_2$O)$_2$] (7). The Dy(III) ion belongs to the heavy lanthanide ions, and the free-ion ground state, $^6H_{15/2}$, is well separated from first excited state, so only the ground state is thermally populated at room and low temperature, which is very different from the situation of Sm(III) because of the larger spin−orbit coupling for Dy(III), even though both of them have the same number of localized unpaired f electrons.

As can be seen from Figure 8, it is worth noting that the situation of **7** is very different from the above complexes. For the latter complexes, the usual decrease in the value of $\chi_M T$ is observed upon lowering the temperature, while for the former complex **7** $\chi_M T$ versus T curves display a minimum. At 300 K, $\chi_M T$ is equal to 28.54 cm^3 K mol^{-1}, as expected for two isolated Dy(III) ions (28.34 cm^3 K mol^{-1}). When the temperature is lowered, $\chi_M T$ increases very slowly to 50 K ($\chi_M T = 29.30$ cm^3 K mol^{-1}) and then decreases down to 14 K. At this temperature, it reaches a minimum of 28.77 cm^3 K mol^{-1} and then increases dramatically as the temperature is further lowered. The whole profile of the $\chi_M T$ vs T curve is indicative of the occurrence of two conflicting effects. On one hand, the decreases in $\chi_M T$ unambiguously originate in the thermal depopulation of the highest Stark levels resulting from the splitting of the free-ion ground state, $^6H_{15/2}$, by the crystal field, and on the other hand, the antagonist process must be the ferromagnetic interaction between the Dy(III) ions. Interestingly, the ferromagnetic interaction in **7** is obviously different from the situation in the reported homodinuclear Dy(III) complex PcDyPcDyPc* (Pc = dianion of phthalocyanine, Pc* = dianion of 2,3,9,10,16,17,23,24-octabutoxyphthalocyanine), **8**, also with ferromagnetic interaction between Dy(III) ions.[4b] In **8**, there is only one inflection with $T_{min} = 8$ K in the whole profile of the $\chi_M T$ versus T curve, while in **7**, there are two inflections, and the T_{min} is 14 K, which is obviously larger than that of **8**. So the presence of the stronger ferromagnetic interaction between the Dy(III) ions in **7** can be concluded, despite a longer Dy(III)···Dy(III) distance, possible because of the different exchange pathways from **8**.

Optical Spectroscopy. For each complex, the cyano ν(C≡N) stretching vibration occurs at the almost same

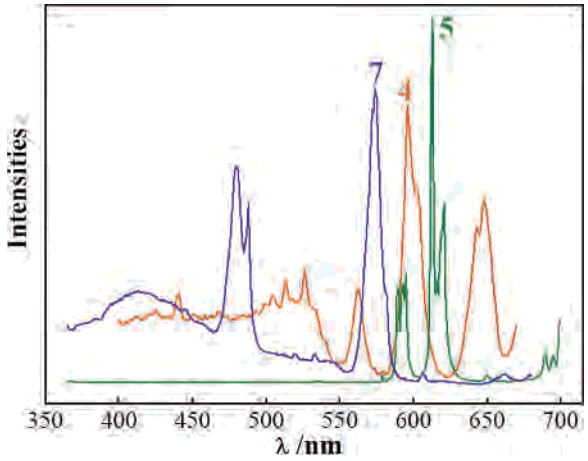

Figure 9. Solid-state emission spectra of **4**, **5**, and **7** (λ_{ex} = 346, 357, and 350 nm, respectively) at room temperature.

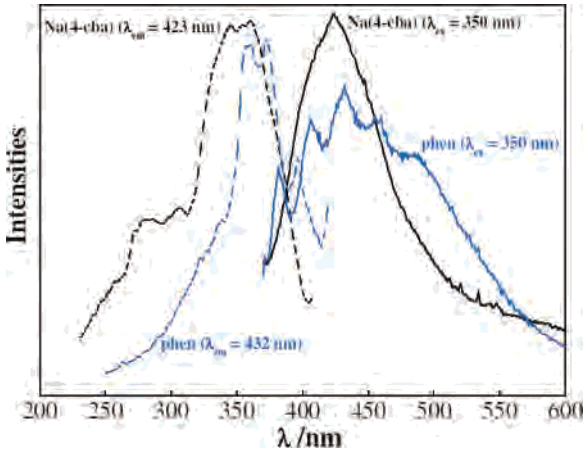

Figure 10. Solid-state excitation (dashed line) and emission (full line) spectra of Na(4-cba) and phen at room temperature.

frequency, ca. 2230 cm^{-1}, as that of the free Na(4-cba), which suggests that the cyano group is not involved in coordination. The asymmetrical and symmetrical stretching frequencies in the carboxylate complexes, $\nu_{asym}(CO_2)$ and $\nu_{sym}(CO_2)$, are sensitive to the carboxylate coordination environments.[21] The terminal carboxylate group in all complexes does not have the typical character of unidentate ligand because of the intervention of the strong bonds, which leads to the difficult discrimination of carboxylate coordination modes. On the whole, both $\nu(CO_2)$ in all complexes are shifted to the higher frequencies relative to values of Na(4-cba).

The luminescence of lanthanide complexes has also attracted intensive research for their high color purity and potentially high internal quantum efficiency.[3,22] It is well-known that the luminescence of lanthanide complexes from the f−f transitions is usually generated via the "antenna effect", since the f−f transition is spin- and parity-forbidden. So we should introduce suitable chromophores in the lanthanide complexes, which absorb light and transfer excitation energy to the lanthanide ions. Aromatic 4-cba and phen ligands, possessing electron-conjugate systems, may be good chromophores for the efficient luminescent sensitization of lanthanide ions. We have measured the photoluminescence spectra of solid samples of **4**, **5**, and **7** at room temperature upon photoexcitation at 346, 357, and 350 nm, respectively, as shown in Figure 9.

The emission peaks of **5** at 579, 592, 613, 650, and 695 nm can be assigned to $^5D_0 \rightarrow {}^7F_J$ (J = 0, 1, 2, 3, 4) transitions of the Eu(III) ion, respectively. Notably, the $^5D_0 \rightarrow {}^7F_2$ transition is much more intense than the $^5D_0 \rightarrow {}^7F_1$ transition, which reflects a low symmetry of the Eu(III) site, consistent to the distorted square antiprism coordination environment. The emission peaks of **4** at 563, 596, and 648 nm can be assigned to $^4G_{5/2} \rightarrow {}^6H_J$ (J = 5/2, 7/2, 9/2) transitions of the Sm(III) ion, respectively, while the emission bands for **7** at 480 and 574 nm can be assigned to $^4F_{9/2} \rightarrow {}^6H_J$ (J = 15/2, 13/2) of the Dy(III) ion. The crystal-field splitting is clearly present in most of all transitions. Interestingly, in the emission of **5**, the ligands-centered emission bond vanished completely, as compared with the ligand-centered emission of pure 4-Hcba and phen ligands (see Figure 10), while in the emission of **4** and **7**, the ligands-centered emission is most quenched, indicating that the ligand-to-Ln(III) energy transfer may be more efficient for **5**. Notable radiationless deactivation, caused by the coordinated water,[23] can be avoided to promote efficient fluorescent emission.

The use of phen-functionalized organic compounds in promoting lanthanide ions emitting intense luminescence has been reported.[24] Actually, deduced from the absorption and emission spectra of Na(4-cba) and phen (Figure 10), the lowest-lying triplet excited energy level (E_T) of Na(4-cba) is close to that of phen. The E_T level of phen can be estimated to be at 21 640 cm^{-1}. The lowest- lying excited energy levels of Sm(III) Eu(III) and Dy(III) are 18 200, 17 500, and 21 100 cm^{-1}, respectively.[24a] Thus, efficient ligand−Ln(III) energy transfer can take place for complexes **4**, **5**, and **7**; 4-cba complexes may act as good candidates for efficient luminescent materials.

Conclusions

In summary, the syntheses and crystal structures of a series of homodinuclear lanthanide complexes containing the 4-cba ligand have been reported, and their magnetic and luminescent properties have been discussed. Two structural types with parallelogramic $[La_2O_2]$ and paddle-wheel-like $[Ln_2(CO_2)_4]$ molecular frameworks have been revealed. Ferromagnetic interactions can be unambiguously found in the Dy(III) complex (**7**) from the profile of $\chi_M T$ versus T curve, while the Gd(III) complex (**6**) is found to be paramagnetic, even though both have comparable Ln(III)···Ln(III) distances. It is worth noting that the ferromagnetic interaction

(21) Deacon, G. B.; Phillips, R. J. *Coord. Chem. Rev.* **1980**, *33*, 227.
(22) Richardson, F. S. *Chem. Rev.* **1982**, *82*, 541.
(23) (a) Haas, Y.; Stein, G. *J. Phys. Chem.* **1971**, *75*, 3677. (b) Stein, G.; Wurzberg, E. *J. Chem. Phys.* **1975**, *62*, 208.
(24) (a) Quici, S.; Cavazzini, M.; Marzanni, G.; Accorsi, G.; Armaroli, N.; Ventura, B.; Barigelletti, F. *Inorg. Chem.* **2005**, *44*, 529. (b) Quici, S.; Marzanni, G.; Forni, A.; Accorsi, G.; Barigelletti, F. *Inorg. Chem.* **2004**, *43*, 1294. (c) Lenaerts, P.; Storms, A.; Mullens, J.; D'Haen, J.; Görller-Walrand, C.; Binnemans, K.; Driesen, K. *Chem. Mater.* **2005**, *17*, 5194. (d)Lenaerts, P.; Driesen K.; Van Deun, R.; Binnemans, K. *Chem. Mater.* **2005**, *17*, 2148.

between the Dy(III) ions in **7** is much stronger than that in the reported homodinuclear Dy(III) complex with ferromagnetic interaction. For the other four complexes (**2**−**5**), the magnetic susceptibility, $\chi_M T$, decreases when the temperature is lowered. However, ferromagnetic or antiferromagnetic interactions cannot be concluded because of the concurrence of the effects of the crystal field and spin−orbital coupling. Notably, a least-squares fitting of $\chi_M T$ versus T of **4** and **5**, deduced from equation for the Sm(III) and Eu(III) ions, respectively, in monomeric system with free-ion approximation, leads to $\lambda = 216(2)$ cm^{-1} for Sm(III) and $\lambda = 404(2)$ cm^{-1} for Eu(III). The emission spectra demonstrate that the 4-cba complexes, especially **5**, might be good candidates for efficient luminescent materials without the quenching effects of coordinated water molecules.

Acknowledgment. We gratefully acknowledge the financial support of the NSF for Distinguished Young Scientist of China (20425104) and the NSF of Fujian Province (A0420002 and 2005I017).

Supporting Information Available: Crystallographic data for **1**−**7** in CIF format, the figures of the coordination geometry of La(III) and Pr(III), the chain structure of **1**, and the layered structure of **2**, infrared spectra of Na(4-cba) and **1**−**7**, excitation and emission spectra of **4**, **5**, and **7**, and XRPD diagrams of **3** and **6**. This material is available free of charge via the Internet at http://pubs.acs.org.

IC0602603